Development of methods to deconvolve data from instrumental devices: Application to acoustic experiments

Henri-Pierre Valero, Stéphanie Gautier, Ginette Saracco, Matthias Holschneider

IEEE Intern. Workshop on Intelligent Signal Processing
Budapest, Hungary, May 24-25, 2001
IEEE - WISP, pp. 159-164, 2001

Development of methods to deconvolve data from instrumental devices: Application to acoustic experiments.

H-P Valero
Schlumberger K.K., Sonic Interpretation
Interpretation Product Line
2-2-1 Fuchinobe, Sagamihara-shi
Kanagawa-ken, 229-0006, Japan.
valero@fuchinobe.skk.slb.com

S. Gautier, G. Saracco, M. Holschneider
CNRS-UMR 6118, Géophysique Interne
Campus de Beaulieu, bât 15
F-35042 Rennes cedex, France
stephanie.gautier@univ-rennes1.fr
ginet@univ-rennes1.fr
hols@univ-rennes1.fr

Abstract

We propose two methods to deconvolve experimental data from the distorsions introduced by the instrumental devices. If we suppose the total acquistion system (emission-reception line, amplifier, pre-amplifier) as a global experimental filter, we can define it experimentally from the generation of a family of source signals dilated in time. The estimation of this filter allows us to deconvolve the recorded output signal. The first approach is based on the simple reconstruction formula of the continuous wavelet transform. The second method is based on the construction of a normalized family of a finite number of specific filters, independent of the frequency range used. In both case, experimental results in an acoustic tank are presented. We show that after deconvolution, the source signal is correctly reconstructed from the recorded output signal and the global instrumental filter.

1. Introduction

A signal measured by an instrumental device can be represented by the following equation:

$$O(t) = (F_{ins} * m * I)(t) \quad (1)$$

where F_{ins} corresponds to the response of the instrumental device, m to the impulse response of the medium and I to the input signal sent by the generator to the experimental system. O is the propagated signal measured by the receiver.

The problem to solve is therefore the following: Is it possible to get back the input signal $I(t)$ in abstaining oneself from the effects of the different measurement devices. In fact, it is the same than doing the contrary operation of the equation (1) that means a deconvolution.

Numerous deconvolution methods dealing with different problems and input parameters of the system exist ([1]-[4],[6]-[8],[11]). The most robust method is the one of Wierner-Levinson ([5],[10]), where the filter is defined by the minimization of a quadratic form : the measurement error in the sens of least squares method. Our approach consists first to build the global instrumental response of our device, in the case of a test medium, then to apply its inverse to the measured output signals. These methods have been applied in real acoustic experiments for low ultrasound frequencies with omnidirectional transducers, and high ultrasound frequencies with plan directional transducers. We will present the calculated filters as well as the deconvolved data of the instrumental response of the devices for two kinds of source-signals.

2. Experimental conditions

We have an acoustic tank in which one we do different propagation experiments. The scheme of the experiment is presented Fig 1. Figure 2 shows the comparison between the theoretical signal emitted in the medium and the one recorded after having crossed our devices.

We can see that the device has an instrumental response variable with respect to the frequency range of the generated signal. The water leads only to a time-delay dephasing, without dispersion effect, but the geometrical divergence for omnidirectional transducer is considered, just as a weak absorption of sound during the travel of the wave between the two kinds of transducers.

Although all sensors have a limited frequency range, we have to choice this range in accordance to the geometrical and mechanical parameters that we want studied in real experimental applications. We need to keep a constant ratio between the geometrical dimensions and the wavelenght of the source, if we want to transpose in acoustic laboratory experiments, real experimental conditions. For examples

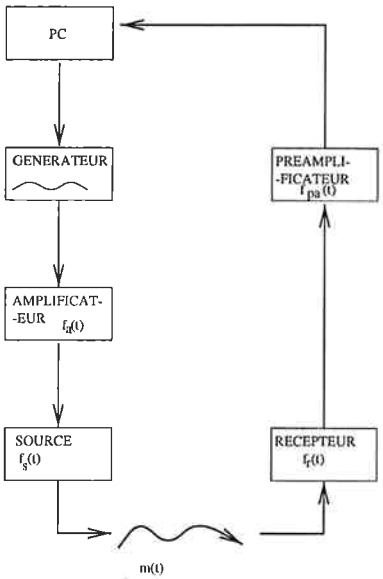

Figure 1. Scheme of the experimental set-up in the water-tank.

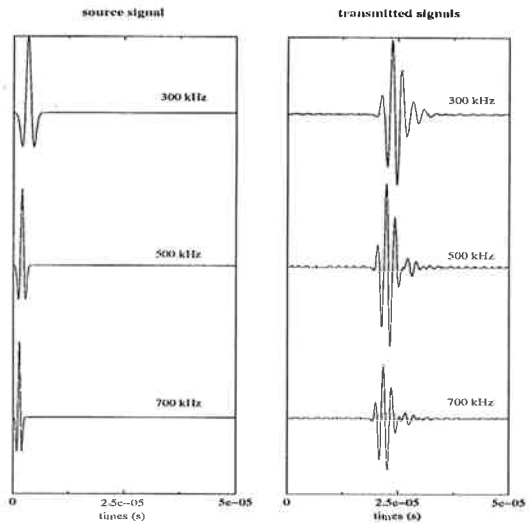

Figure 2. Comparison of emitted source signal (left) and received signal after crossing the experimental dispositif (right).

examples the size of heterogeneities in front of the emitted wavelenght in diffusion problem or the distance between the scatterer or the source with regard to the receiver in propagation or scatering problem. Moreover, a transposition in low ultrasound frequencies implies multiple parasite reflections on the walls of the acoustic tank. These waves can be partially attenuated with the help of alveoled and conics absorbers (latex or polyethyrene material mixed to hight density composites). In geoexploration experiments the frequency range currently used is around 0.1Hz-10kHz. This corresponds to a wavelenght transposition of 100m-1dm in the acoustic tank respectively to a water mean velocity of 1500m/s. To keep a constant ratio between the physical phenomena to be analyzed and experimental geometric parameters, we need to work in a frequency range of 10Hz-1MHz. The limitations on one hand of tank dimensions and on the other hand of the piezo-electric technology imply to work with two kinds of ultrasound source. A signal limited to a frequency-range of 20kHz-140kHz (omnidirectional transducer) and to ultrasound-range 100kHz-1MHz (directional transducer). This corresponds to a global wavelenght of 15cm to 0.15mm.

3 Methods of deconvolution

3.1. first method

If $S(b,a)$ are the wavelet coefficients of the global instrumental filter $F_{ins}(t)$ associated to a dilated family of "wavelet-source" signals $(D^a I)(t)$, we can write under some conditions ([9]) an exact formula allowing us to reconstruct for each time τ the global filter:

$$F_{ins}(\tau) = R_e\left[K_I \int_0^{+\infty} S(\tau, a)\,\frac{da}{a}\right] \qquad (2)$$

where K_I is a non nul constant defined by $K_I = \int_0^{+\infty} \frac{\hat{I}^*(\omega)}{\omega} d\omega$. I^* is the complex conjuguated of the analyzing wavelet I such that $S(b,a) = \left(F * D^a \tilde{I}\right)(b)$, with $\tilde{I}(t) = I^*(-t)$.

The instrumental filter expression in this discrete form is then:

$$F_i(t) = K_g \sum_{n=\min}^{\max} S_{F_n}(t, a_n)\,\frac{\Delta a_n}{a_n}, \qquad (3)$$

where min and max correspond to the minimal and maximal value of the emitted frequency. The fact of being limited on the number of dilation parameters may lead to a loss of information during the reconstruction of the filter. Nevertheless, it is necessary to apodise $\hat{I}^*(\omega)$ to obtain a good result in the time domain. This method easy to apply depends on the frequency range of the generated input signals. A necessary condition for the reconstruction is to generate a wavelets family with a scale-range of 3 octaves, decomposed linearly into 10 voices (linear intervals). It means that the result depends on the number of wavelets generated. Nevertheless the results of the deconvolution with an apodistion window show that the source signal is correctly reconstructed from the recorded transmitted signal and the instrumental global filter (see Figures 3 and 4). These results are obtained in low ultrasound frequencies

with omnidirectional hydrophones for two different transient signals a ricker function (derivative of second order of a Gaussian function) and a Morlet's wavelet (modulated Gaussian). The number of octaves of the dilation parameters is close to three (40-140kHz). We can observe a weak difference in the amplitude between the input signal A and the reconstructed signal C. Nevertheless the waveforms are correctly rebuilt.

3.2. Extended method

Let us denote in Fourier space a general family of filters of controlled input signals $\hat{I}_n(u)$. After passage through the acquisition system we obtain, as previously, the measurements:

$$\hat{O}_n(u) = \hat{F_{ins}}(u)\hat{I}_n(u).$$

Instead of recovering $\hat{F}(u)$ we can only hope to obtain $\hat{\chi}(u)\hat{F}(u)$, where $\hat{\chi}(u)$ is a suitable window function that we can choose such that $\sum_n(\hat{h}_n * I_n)(t) = \chi(t)$. We are looking for a solution:

$$\hat{\chi}(u)\hat{F_{ins}}(u) = \sum_n \hat{h}_n(u)\,\hat{O}_n(u).$$

The filters h_n should be regular in order to obtain stable inversions. A solution to this problem is obtained by setting

$$\hat{h}_n(w) = \frac{\hat{I}_n^*(w)}{\sum_m \left|\hat{I}_m(w)\right|^2} \times \hat{\chi}(w). \qquad (4)$$

The main point is the choice of the function $\hat{\chi}$ which plays an important role in the stability of calculus. This choice will be made by studying the behavior of the ratio:

$$\frac{\hat{\chi}(u)}{\sum_m \left|\hat{I}_m(u)\right|^2}$$

The signal deconvolved for the voice n will be calculated as following:

$$\hat{O}_n^d(u) = \hat{F}_{inv}(u)\,\hat{O}_n(u). \qquad (5)$$

where

$$\hat{F}_{inv}(u) = \frac{\hat{\chi'}(u)}{\hat{F}_{int}(u)} \qquad (6)$$

where $\hat{\chi'}(u)$ is an adapted function deduced from $\hat{\chi}(u)$ allowing us to limit the numerical instabilities (division by zero). The deconvolved signal verifies:

$$\hat{O}_n^d(u) = \frac{\hat{\chi'}(u)}{\hat{O}_n(u)} \qquad (7)$$

So, we dispose in fact of a very general method of the construction of a filter appropriate to the experiment regardless of the input signal and the used frequency range.

4 Application to acoustic data

Experiments are performed in the frequency range of 40kHz-140kHz with omnidirectional transducers and appropriated amplifier and pre-amplifier for the first method, and around 200kHz-900kHz with directional transducers for the extended method. The source signals emitted in the water tank are respectively a Morlet's wavelet:

$$g(t) = \cos(u_0 t)\exp\left(-\frac{t^2}{2\sigma^2}\right), \qquad (8)$$

and a ricker:

$$r(t) = \left(1 - 2(\pi f t)^2\right)\exp\left(-\pi f t\right)^2 \qquad (9)$$

The results of the deconvolution in the case of the first method are shown (Fig. 3). The signal A corresponds to the output signal, B is the source signal generated by the synthetizer and send to the emitter. C is the result of the deconvolution. The phasis and the modulus of the global instrumental filter is presented Fig.(4) for an omnidirectional source and low frequencies. The deconvolution examples based on the extended method for omnidirectional transducers with a family of Morlet's function (left) and ricker function (right)is shown Fig.5 with the same notation for the curves A,B,C than 3. In this case, the amplitude and the waveform of the reconstructed signals C are in perfect concordance with the emitted signal A.

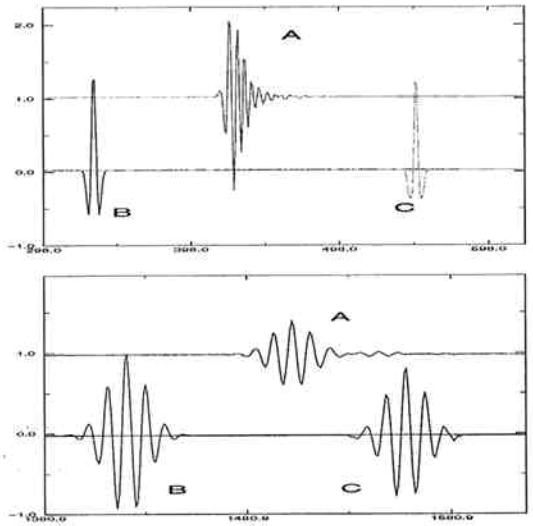

Figure 3. Deconvolution examples for a ricker (top) and a Morlet's wavelet (bottom) using the simple reconstruction formula of the C.W.T (first method). The curves represent respectively A: the signal measured to the receiver after crossing the experimental dispositif, B: the source signal and C: the rebuilt signal.

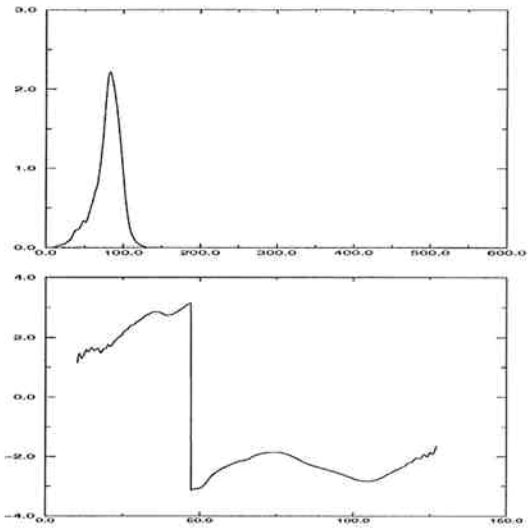

Figure 4. Modulus and phase of the instrumental filter using the simple reconstruction formula of the continuous wavelet transform (first method).

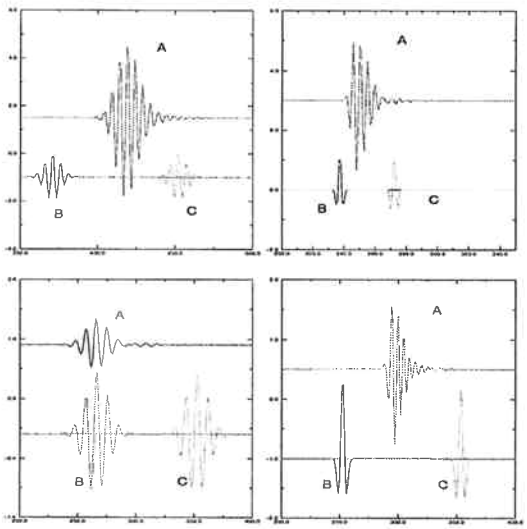

Figure 5. Deconvolution examples based on the general method for a ricker (right) and a Morlet's wavelet (left), for two different frequencies. The variation between the recorded signal, for two differents frequencies, confirms the necessity to deconvolve data of the instrumental filter.

For directional transducers, the results of the deconvolution are presented with a ricker source signal of central frequency $fc = 300kHz$ (Fig.6) and $fc = 500kHz$ (Fig. 7). The associated global instrumental filter is shown Fig.9.

The family of ricker's function are generated by linear step of 20kHz in the frequency range 200kHz-900kHz. Thoses frequencies cover the band pass of transducers centred on 500kHz. The acquistion parameters are fixed during all the experiment (sampling frequency, voltage calibration, power gains for amplifier and preamplifier,..). Consequently, the differences obtained between the source emitted and the propagated signal measured to the receiver are only due to the global filter of the experimental devices.

The initial $\hat{\chi}(u)$ function used for the determination of the individual filters $\hat{h_n}(u)$ are presented Fig. 10 in appendix. The adapted function $\hat{\chi'}(u)$ deduced from the $\hat{\chi}(u)$ function to limit numerical instability in the computation of the $\hat{h_n}(u)$ filters are presented Fig. 8 for two kinds of window, the $\hat{\chi}(u)$ function and a rectangular window.

The figure 9 is the computed global filter of the experimental devices. The inverse global filter is then applied to the recorded sgnals in order to remove the effect of the instrumental filter from data. The comparisons between the experimental results (source signal convolved with the $\hat{\chi'}(w)$'s function) and the theoreticals ones are both in time and frequency domain, in a perfect concordance (see Fig. 6 and 7). Some small high frequencies oscillations are

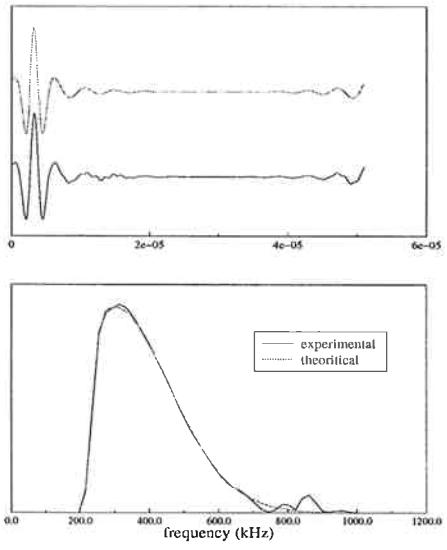

Figure 6. Results from the deconvolution of recorded signal with inverse instrumental filter in time (top) and frequency (bottom) domain for the frequency source of 300 kHz.

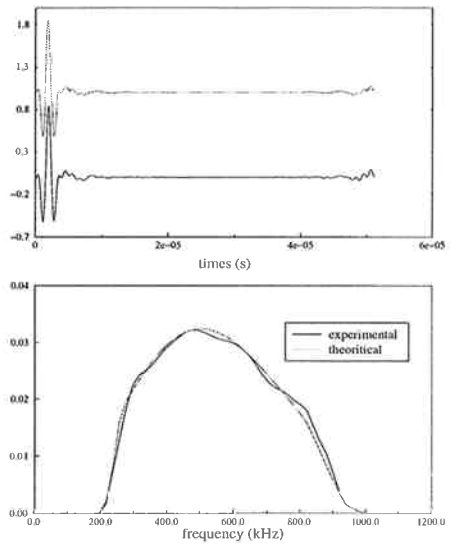

Figure 7. Results from the deconvolution of recorded signal, in time (top) and frequency (bottom) domain for the frequency source of 500 kHz.

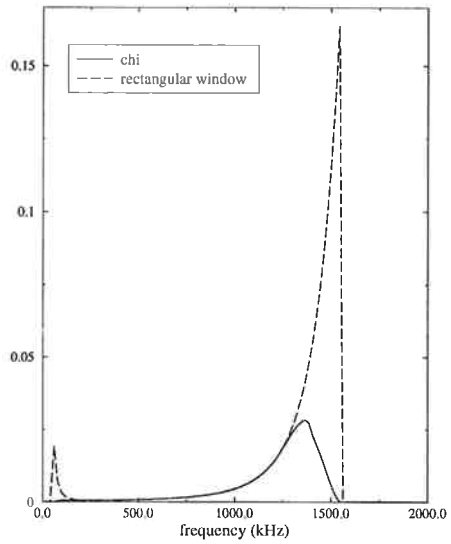

Figure 8. Ratio modulus $\frac{\widehat{W}(w)}{\sum_m \left|\widehat{I_m}(w)\right|^2}$ for two kinds of window $\widehat{W}(w)$: the function $\widehat{\chi}(w)$ and a rectangular window with the same width. The regular behaviour of the ratio when the window is the function $\widehat{\chi}(w)$ indicates that the numerical instabilities are more limited that if we use the recangular one.

6 and 7). Some small high frequencies oscillations are presents in curves A. We can associate these small oscillations to the convolution of the transmitted signals with the inverse filter whose modulus reaches a maximum for these values. This method is nevertheless very effecient considering the weak differences between theoritical and rebuilt signals

We notice that the methods of deconvolution are efficient independently of the emitted signal (Morlet or ricker functions), space distribution (directivity pattern of tranducers), and for the last method independently of the frequency range of the source signal.

5 Conclusion

These methods presented to build the global instrumental filter are easy to implement from an experimental point of view as well as from a numerical one. They give similar results. The first one, based on the wavelet theory and more precisely on the simple reconstruction formula of the wavelet transform depends on dilations range generated. It means that the amplitude of the reconstructed signal can be lower than the emitted signal, because we need to have a minimum frequency range of three octaves during experiments. These conditions limit the efficiency of this method in laboratory experiments, in particular in acoustic tank. The second one, more general, is based on a family filter construction that enables to free ourselves from the work frequency range.

Acoustical experiments have shown the validity of both methods because of the good deconvolution of measured output signals. A new interest is the use of the presented methods to compute more general filters for example, of an object inserted in the middle of the tank.

6 appendix

The function $\hat{\chi}(u)$ used for the determination of the individual filters $\hat{h_n}(u)$ is initialized with a phase zero and an amplitude modulus of one. The characteristics of this function are presented Fig. 10. The rebuilt function $\hat{\chi}(u)$ using rickers as recorded family functions in the computation of the global filter is presented in phase and modulus Fig.11.

References

[1] A.J. Berkhout, Least-squares inverse filtering and wavelet deconvolution, *Geophysics*, 42, 1369-1383, 1977.

[2] N. Ott and H.G. Meder, The Kalman filter as prediction error filter, *Geophysical Prospecting*, 20, 549-560, 1972.

[3] K.L. Peacok and S. Treitel, Predictive deconvolution: Theory and practice, *Geophysics*, 34, 155-169, 1969.

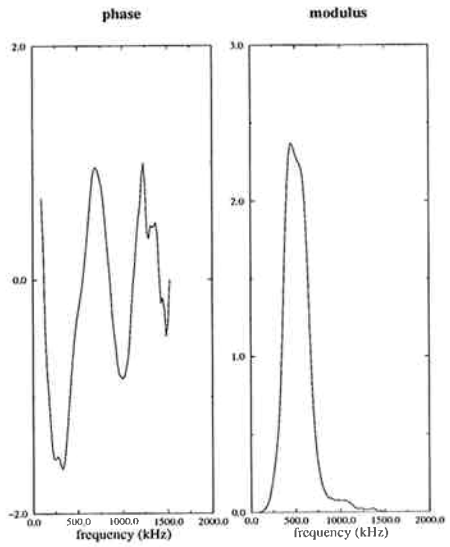

Figure 9. Phase and modulus of the computed global instrumental filter.

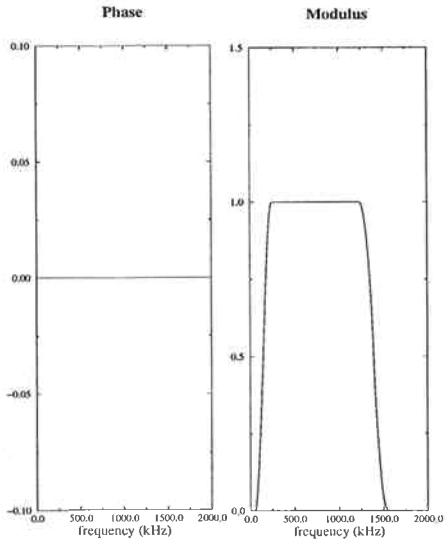

Figure 10. Phase and modulus of the function $\widehat{\chi}(w)$ used in the calculations.

[4] S. Treitel and L.R. Lines, Linear inverse theory and deconvolution, *Geophysics*, 47(8), 1153-1159, 1982.

[5] A. Jurkevics and R. Wiggins, A critique of seismic deconvolution methods, *Geophysics*, 49(12), 2109-2116, 1984.

[6] N.G. Paulter, A causal regularizing deconvolution filter for optimal waveform reconstruction, *IEEE - Trans. Instrum. Meas.*, 43(5), apr. 1996.

[7] S. Roy and M. Souders, Non-iterative waveform deconvolution using analytic reconstruction filters with time-domain weighting, *17th IEEE - Inst. Measur. Tech. Conf.*, 3, 1429-1434, 2000.

[8] T.J. Ulrych, Application of homomorphic deconvolution to seismology, *Geophysics*, 36, 650-660, 1971.

[9] G. Saracco and Ph. Tchamitchian, Retrieval of a time-dependent source in an acoustic propagation problem, *Inv. Prob. in Act. (Inv. Prob. and Theore. Imag.)*, Edt. P.C Sabatier, Springer-Verlag, 207-211, 1990.

[10] E.A. Robinson and S.A. Treitel, Principles of digital Wiener filtering, *Geophysical prospecting*, 15, 311-333, 1967.

[11] Wiggins R. Minimum entropy deconvolution. *Geoexploration*, 16, 21-35, 1978.

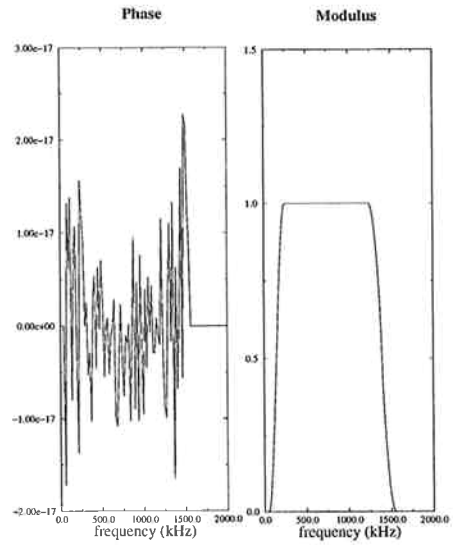

Figure 11. Phase and modulus of the function $\widehat{\chi}(w)$ rebuilt using rickers as recorded data in the computation of the global filter.